0026-895X/04/6603-368–376$20.00
MOLECULAR PHARMACOLOGY
Copyright © 2004 The American Society for Pharmacology and Experimental Therapeutics
Mol Pharmacol 66:368–376, 2004

Vol. 66, No. 3
3160/1168508
Printed in U.S.A.

COX-2 Regulates the Insulin-Like Growth Factor I–Induced Potentiation of Zn^{2+}-Toxicity in Primary Cortical Culture

Joo-Young Im, Doyeun Kim,[1] Kang-Woo Lee, Jung-Bin Kim, Ja-Kyeong Lee, Dong Sik Kim, Young Ik Lee, Kwon-Soo Ha, Cheol O Joe, and Pyung-Lim Han

Department of Neuroscience, Neuroscience Research Center and Medical Research Institute, Ewha Womans University School of Medicine, Seoul, 110-783, Korea (J.-Y.I., D.K., K.-W.L., P.-L.H.); Department of Biological Sciences, Korea Advanced Institute of Science Technology, Daejon, 305-701, Korea (D.K., C.O.J.); Department of Anatomy, Inha University School of Medicine, Inchon, 400-712, Korea (J.-B.K., J.-K.L.); Liver Cell Signal Transduction Lab., Bioscience Research Division, Korea Research Institute of Bioscience and Biotechnology, Daejeon, 305-333, Korea (D.S.K., Y.I.L.); Department of Molecular and Cellular Biochemistry, Kangwon National University School of medicine, Chunchon, 200-701, Korea (K.-S.H.)

Received December 15, 2003; accepted May 13, 2004

This article is available online at http://molpharm.aspetjournals.org

ABSTRACT

The pretreatment of cultured cortical neurons with neurotrophic factors markedly potentiates the cytotoxicity induced by low concentrations of Zn^{2+} or excitotoxins. In the current study, we investigated the mechanism underlying the insulin-like growth factor-I (IGF-I)-induced Zn^{2+} toxicity potentiation. The pretreatment of primary cortical cultures for more than 12 h with 100 ng/ml of IGF-I increased the cytotoxicity induced by 80 μM Zn^{2+} by more than 2-fold. The IGF-I–enhanced cell death was blocked by the COX-2–specific inhibitors *N*-[2-(cyclohexyloxyl)-4-nitrophenyl]-methane sulfonamide (NS-398; 10–100 μM) and 1-[(4-methylsulfonyl)phenyl]-3-trifluoro-methyl-5-[(4-fluoro)phenyl]pyrazole (SC58125; 10 μM) and by the antioxidant trolox (30 μM). In addition, it was observed that COX-2 expression was increased 12 to 24 h after IGF-I treatment. Preincubation of cortical cultures with IGF-I increased arachidonic acid (AA)-induced cytotoxicity, and AA increased Zn^{2+} toxicity, which suggested the involvement of COX activity in these cellular responses. Moreover, enhanced COX-2 activity led to a decrease in the cell's reducing power, as indicated by a gradual depletion of intracellular GSH. Cortical neurons pretreated with IGF-I and then Zn^{2+} showed consistently enhanced reactive oxygen species production, which was repressed by NS-398 and SC58125. Cortical neurons treated with Zn^{2+} and then AA displayed the increased ROS production, which was also suppressed by NS-398 and SC58125. These results suggest that COX-2 is an endogenous factor responsible for the IGF-I–induced potentiation of Zn^{2+} toxicity and that enhanced COX-2 activity leads to a decrease in the cell's reducing power and an increase in ROS accumulation in primary cortical cultures.

Neurotrophic factors such as nerve growth factor, BDNF, NT-3, and IGF-I play a critical role in cell proliferation, survival, and neurite outgrowth during neuronal development. They also produce neuroprotective effects against various neural injuries, including ischemia, trauma, and Alzheimer's disease (Wu and Pardridge, 1999; Nabeshima and Yamada, 2000; Namiki et al., 2000; Guan et al., 2001). Under certain conditions, however, neurotrophic factors produce cytotoxic effects. Pretreatment for 24 h with various neurotrophins, such as BDNF and NT-4/5, markedly potentiates the necrotic cell death of primary cortical neurons induced by oxygen-glucose derivation or NMDA (Koh et al., 1995; Behrens et al., 1999; Lobner and Ali, 2002). Moreover, the preincubation of cultured cortical neurons with BDNF increases their sensitivity to excitotoxicity through the activation of phosphoinositide-3 kinase and the induction of nNOS or TrkB (Samdani et al., 1997; Fryer et al., 2000; Kim et al., 2003b). BDNF increases the excitotoxic cell death of hippocampal neurons by inducing NMDA receptor subunits (Prehn, 1996; Small et al., 1998; Glazner and Mattson, 2000) and potentiates free radical-mediated injury or NO donor-induced apoptosis in primary cortical cultures (Gwag et al.,

J.-Y.I. and D.K. contributed equally to this work.
[1] Current address: Hanhwa Institute of Medicinal Chemistry and Life Science, Daejeon, Korea.

ABBREVIATIONS: BDNF, brain-derived neurotrophic factor; IGF, insulin-like growth factor; NMDA, *N*-methyl-D-aspartate; NNOS, neuronal nitric-oxide synthase; KA, kainic acid; NT-4/5, neurotrophin-4/5; BSO, L-buthionine sulfoximine; COX, cyclooxygenase; ROS, reactive oxygen species; DIV, days in vitro; LDH, lactate dehydrogenase; PG, prostaglandins; AA, arachidonic acid; CM-H_2DCFDA, 5-(and-6)-chloromethyl-2′,7′-dichlorodihydrofluorescein diacetate; NS-398, *N*-[2-(cyclohexyloxyl)-4-nitrophenyl]-methane sulfonamide; SC58125, 1-[(4-methysulfonyl)phenyl]-3-tri-fluoromethyl-5-(4-fluorophenyl) pyrazole; DPI, diphenylene iodonium; NOS, nitric oxide synthase; SC560, 5-(4-chloro-phenyl)-1-(4-methoxy-phenyl)-3-trifluoromethylpyrazole.

1995; Ishikawa et al., 2000). Consistent with these observations, BDNF and NT-4/5 exacerbate the injury induced by kainic acid (KA) in pyramidal neurons of the CA3 region (Rudge et al., 1998), and free radical-induced neuronal necrosis in vivo (Won et al., 2000).

As is required for BDNF-induced potentiation, IGF-I potentiation requires new protein synthesis. IGF-I pretreatment aggravates Fe^{2+}- or BSO-mediated injury in cortical neurons, a process that involves the up-regulation of phosphoinositide-3 kinase and/or extracellular signal-regulated kinase activation (Gwag et al., 1995; Fryer et al., 2000). Thus, IGF-I–induced potentiation seems to have features distinct from those of BDNF and NT-4/5. Although IGF-I–induced potentiation might occur through a mechanism that involves the altered activations and/or enhanced expressions of genes, which make neuronal cells highly vulnerable to subsequent or concurrent cytotoxic stress, the detailed mechanism underlying IGF-I–induced potentiation remains ill-defined.

A number of previous studies have reported that COX-2 activation leads to neuronal cell death via neuroinflammation (Vane et al., 1998; Kyrkanides et al., 2002). The COX-2–selective inhibitors, NS398 and SC58125, reduced the production of prostaglandin E2 and the neuronal loss in the models of middle cerebral artery occlusion (Nogawa et al., 1997) and global ischemia (Nakayama et al., 1998). Nonetheless, there is a growing body of evidence, albeit indirect, suggesting that COX-2 might be involved in ROS generation. For example, KA-induced damage in the rat hippocampus reduced the GSH content and increased lipid peroxidation, both of which were attenuated by the COX-2–specific inhibitor, nimesulide (Candelario-Jalil et al., 2000). In cerebellar granule cells, the COX inhibitor indomethacin blocked NMDA-, KA- and cyanide-induced ROS production. Moreover, pretreatment with the COX-2 inhibitor, NS398, significantly decreased the generation of ROS in response to KCN injury (Gunasekar et al., 1998; Boldyrev et al., 1999). However, these studies did not answer the question as to whether COX-2 plays a role in the generation of ROS in neuronal cells directly or indirectly, thus failing to reveal the manner in which COX-2 is involved in generating ROS stress. As a result, the detailed mechanism and the conceptualization of the role of COX-2 in ROS generation require further substantiation.

Free Zn^{2+} is an important mediator of neurodegeneration in various pathological conditions (e.g., ischemia, seizure, trauma, and Alzheimer's disease) (Frederickson et al., 1988; Koh et al., 1996; Suh et al., 2000; Lee et al., 2002; Cho et al., 2003). Excessive release of synaptic Zn^{2+} and the subsequent Zn^{2+} overload in neurons triggers neuronal cell death (Assaf and Chung, 1984; Frederickson et al., 1988; Koh et al., 1996). This Zn^{2+} overload increases the levels of ROS and lipid peroxidation in primary cortical neurons (Kim et al., 1999a,b). Zn^{2+} overload also induces NADPH oxidase, and subsequent ROS accumulation in cortical neurons and glia (Noh et al., 1999; Noh and Koh, 2000). Moreover, exposure to Zn^{2+} induces NAD^+ depletion, GAPDH inhibition, progressive ATP reduction, and subsequent neuronal death (Sheline et al., 2000). Thus, free Zn^{2+} plays a critical role in neuronal cell death during various pathological conditions in vivo. In the current study, we demonstrate that pretreatment with IGF-I increases COX-2 expression, which leads to ROS up-regulation and potentiates cytotoxicity in primary cortical cultures.

Materials and Methods

Preparation of Mixed Cortical Cultures and Drug Treatment. Mixed cortical cells were cultured as described previously (Cho et al., 2003). They were prepared from embryonic day 15.5 (E15.5) ICR mouse cortices. Dissociated cortical cells were plated in minimal essential medium supplemented with 20 mM glucose, 5% fetal bovine serum, 5% horse serum, and 2 mM glutamine at a density of 5 hemispheres/plate (approximately 2×10^5 cells per well) in poly-D-lysine (100 μg/ml) and laminin (4 μg/ml) coated 24-well plates, and maintained at 37°C in a humidified 5% CO_2 incubator. At day 6 in vitro (DIV6), when the astrocytes reached confluence underneath the neurons, cytosine arabinofuranoside was added to a final concentration of 10 μM and maintained until DIV8 to halt glial growth. Fetal bovine serum and glutamine were not added, but instead the culture medium was supplemented with 10% horse serum from day 6. The medium was changed twice weekly after day 8. The cortical cultures at DIV13–15 were used for the Zn^{2+} and other toxicity studies.

To preincubate cortical neurons with IGF-I, mixed cortical cultures were washed three times with serum-free medium and incubated with varying doses of IGF-I for 6, 12, 18, and 24 h or for the designated times. For Zn^{2+} treatment, cortical cultures were washed three times with HEPES-buffered salt solution (120 mM NaCl, 5.4 mM KCl, 0.8 mM $MgCl_2$, 1.8 mM $CaCl_2$, 20 mM HEPES, 10 mM NaOH, and 15 mM glucose) and then incubated with HEPES-buffered salt solution with varying doses of $ZnCl_2$ for 30 min at room temperature. Exposure to Zn^{2+} was terminated by washing cultures three times with serum free medium. Cultures were then maintained in serum-free medium until required for analysis. Cell death was determined 24 h after Zn^{2+} treatment unless otherwise indicated.

Assessment of Cell Death. Cell death was determined using the lactate dehydrogenase (LDH) assay, as described previously (Cho et al., 2003). In brief, 25 μl of culture medium was transferred to a microplate and 100 μl of NADH solution (0.3 mg/ml NADH and 0.1 M potassium phosphate, pH 7.4) was added to the medium. After 2 min, 25 μl of pyruvate solution (22.7 mM pyruvate and 0.1 M potassium phosphate, pH 7.4) was added. The immediate change of NADH to NAD^+ after this pyruvate addition was determined by measuring absorbance reduction at 340 nm on a SpectraMax microplate reader (Molecular Devices, Sunnyvale, CA). LDH activity was normalized such that sham-treated cultures and complete cell death were counted as 0% and 100%, respectively, and normalized LDH activity was regarded to indicate cell death. Complete cell death was accomplished by treatment with 300 μM glutamate for 24 h. In some experiments, trypan blue staining was used to visualize cell death. In this case, culture medium was removed by aspiration and cells were immersed in 0.04% trypan blue solution for 1 min, washed with HEPES-buffered salt solution, and subjected to microscopic analysis. To visualize the morphological changes of cells during cell death, cortical cultures were stained with anti-MAP-2 (Upstate Biotechnology, Lake Placid, NY).

Immunoblotting. Western blot analysis was carried out as described previously (Lee et al., 1999). In brief, cultures were lysed with ice-cold 150 mM NaCl and 1% Nonidet P-40 in 20 mM Tris-HCl. Protein samples were resolved on 10% SDS-PAGE, and specific signals on the blots were visualized using an enhanced chemiluminescence (ECL) kit (Amersham Biosciences, Piscataway, NJ). Immunoblotting was performed using monoclonal anti-COX-2 antibody (1:80; BD Transduction Laboratories, Lexington, KY).

Immunocytochemistry. Cells were fixed with 4% paraformaldehyde in 0.1 M phosphate buffer, pH 7.4, for 10 to 20 min at room temperature, permeabilized with 0.2% Triton X-100 in PBS containing 5% goat serum (blocking solution) for 1 h, and then reacted with

anti-COX-2 antibody (1:200), anti-COX-1 (Alexis, San Diego, CA; 1:1000), or anti-MAP-2 (1:100; Upstate Biotechnology) overnight. Cells were then incubated with fluorescein- or horseradish peroxidase-conjugated goat anti-mouse IgG [1:100, Sigma, (St. Louis, MO), or 1:1000, Santa Cruz Biotechnology (Santa Cruz, CA)] for 1 h. The peroxidase reaction product was visualized with 0.05% 3′-diaminobenzidine (DAB) in the presence of 0.01% hydrogen peroxide. Stained cells were photographed under a Nikon Eclipse inverted microscope (Nikon, Japan).

Semiquantitative RT-PCR Analysis. RT-PCR was performed as described previously (Estus et al., 1994) with a minor modification. Total RNA was isolated from a cortical culture using Tri reagent, and cDNA was synthesized from 10 μg of the total RNA using Moloney murine leukemia virus reverse transcriptase (First Strand RT kit; Stratagene, La Jolla, CA). PCR reactions were set up in a 50-μl mixture containing 100 μM dATP, dTTP, and dGTP, 50 μM dCTP, 10 μCi of α-[^{32}-P]dCTP (3000 Ci/mmol), 1 μM concentration of each primer, 1× *Taq* buffer, 1 unit of *Taq* (QIAGEN, Valencia, CA), and 1% of the synthesized cDNA. The primer sequences used were 5′-GGA ACA TGG ACT CAC TCA GT-3′ and 5′-GGA GGC ACT TGC ATT GAT GG-3′ for COX-2; 5′-GGA ACA GGC GTC CGT GTT GA-3′ and 5′-CAT CCA CCA GTG CCT CAA CC-3′ for COX-1; and 5′-AGG GCA TCT TGG GCT ACA CTG AGG-3′ and 5′-GTT ATT ATG GGG GTC TGG GAT GGA-3′ for GAPDH. The minimum number of PCR cycles necessary to detect the PCR products was 23 to 25 under the given conditions. After PCR amplification, PCR products were separated on 5% polyacrylamide gel, visualized by autoradiography, and quantified using a Bioimaging Analyzer System (Fuji Film, Tokyo, Japan).

Prostaglandin E2 Release Assay. Cyclooxygenase activity was assayed by measuring prostaglandin E2 (PGE_2) release, the major product of prostaglandin synthesis. Cultures were exposed to IGF-I for 24 h. After incubating with 30 μM arachidonic acid (AA) for 30 min, media were collected to determine PGE_2 release by using the PGE_2 ^{125}I assay system (RPA530; Amersham Biosciences).

ROS Visualization. ROS visualization was performed as described previously (Greenlund et al., 1995). In brief, cultures were incubated for 30 min at 37°C in medium containing 10 μM 5-(and-6)-chloromethyl-2′,7′-dichlorodihydrofluorescein diacetate (CM-H_2DCFDA; Molecular Probes, Eugene, OR). CM-H_2DCFDA is a cell membrane-permeable, redox-sensitive fluorescent dye that is not fluorescent in the reduced state. However, when oxidized by hydrogen peroxide, it is converted into its fluorescent form (Mahadev et al., 2001; Hool and Arthur, 2002). The cultures were washed twice with HEPES buffer and subjected to fluorescence microscopic analysis. Dichlorofluorescein fluorescence was visualized under a Nikon Eclipse inverted microscope (Nikon, Japan) equipped with a 75-W Xenon lamp, a 450- to 490-nm excitation filter, and a 520-nm emission filter; excitation was measured at 504 nm and emission at 529 nm using a spectrofluorometer (Shimadzu, Kyoto, Japan). For quantification purposes, fluorescence levels were measured at three adjacent spots that roughly covered the diameter of each well; these three measurements were averaged and regarded as a data point.

GSH Measurement. GSH concentration was determined as described previously (Kim et al., 2003a). In brief, cortical cultures were incubated for 30 min at 37°C with 100 μM monochlorobimane (Molecular Probes, OR), washed with PBS, and lysed in 0.2% Triton X-100 in PBS. The changes in fluorescence caused by the formation of the GSH-monochlorobimane adduct were determined at 380 nm excitation and 478 nm emission using a spectrofluorometer (Shimadzu).

Results

The Potentiation of Zn^{2+} Toxicity by IGF-I in Cortical Neuronal Culture. We observed that pretreatment of the primary cortical culture for 24 h with 100 ng/ml IGF-I notably enhanced Zn^{2+}-induced cytotoxicity. To explore the mechanism involved, we first determined the dose- and time-dependent effects of IGF-I and Zn^{2+} treatments on cell death using the LDH assay (Fig. 1, A–C). The results of obtained generally agreed with the trypan blue staining results (data not shown) and with the observed morphological changes. Pre-exposing the cortical culture to 30 to 100 ng/ml of IGF-I for more than 12 h greatly aggravated Zn^{2+}-induced neuritic degeneration and somatic cell loss versus the neurons treated with IGF-I or Zn^{2+} alone (Fig. 1D). In essence, the pretreatment of primary cortical culture for 12 to 24 h with 100 ng/ml IGF-I increased the cytotoxic effect of 80 μM Zn^{2+} more than 2-fold (Fig. 1, B–D). Continuous treatment with 100 ng/ml IGF-I proved slightly cytotoxic (Fig. 1B). Unless otherwise indicated, IGF-I was applied at 100 ng/ml for 12 to 24 h and 80 μM Zn^{2+} was treated for 30 min throughout this work.

Increased ROS Was Associated with the IGF-I–Induced Potentiation of Zn^{2+} Toxicity. IGF-I–enhanced Zn^{2+} toxicity was significantly inhibited by 30 μM trolox, indicating that oxidative stress is involved in this process

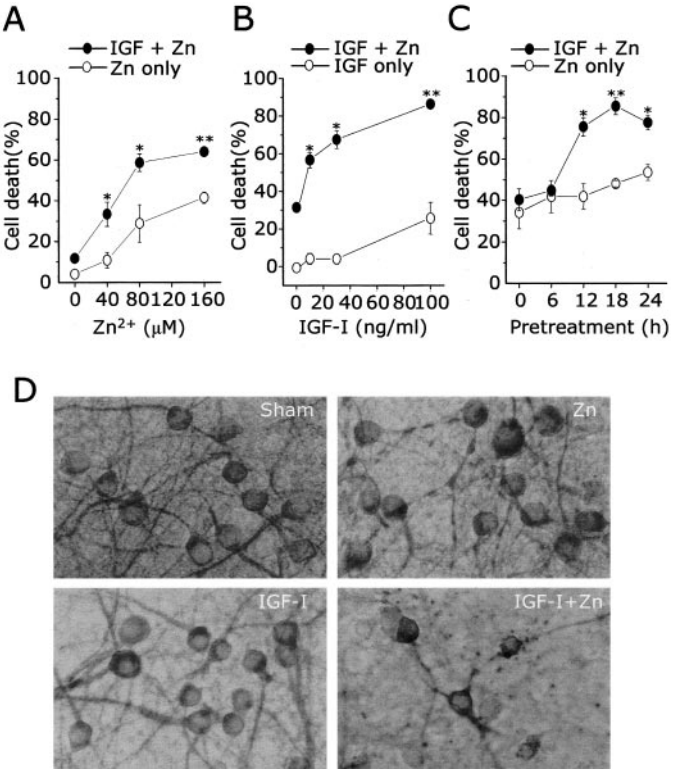

Fig. 1. Characterization of the IGF-I–induced potentiation of Zn^{2+} toxicity in primary cortical neurons. A, cytotoxicity induced by Zn^{2+} was aggravated when cortical cultures were pretreated with 100 ng/ml IGF-I. Zn^{2+} was applied briefly for 30 min throughout this work as described under *Materials and Methods*. Cell death was measured at 24 h after Zn^{2+} treatment. B, IGF-I dose-dependently potentiated Zn^{2+} toxicity. Zn^{2+} (80 μM) was treated for 30 min and cell death was measured 24 h later. C, the strong potentiation of Zn^{2+}-induced cell death necessitated long-term incubation with IGF-I (100 ng/ml). Cell death was measured 24 h after Zn^{2+} treatment. D, photomicrographs of cortical cultures stained with anti-MAP-2 antibody 24 h after Zn^{2+} challenge. Cortical cultures were incubated for 12 h with 30 ng/ml IGF-I followed by treatment for 30 min with 80 μM Zn^{2+} (IGF-I+Zn). Sister cultures treated with 80 μM Zn^{2+} only (Zn) or 30 ng/ml IGF-I only (IGF-I) were prepared. Sham, sham control. * and **, differences at the $p < 0.05$ and $p < 0.01$ levels, respectively, compared with the corresponding control. $n = 8$ to 12 in all cases.

(Fig. 2A). This result prompted us to search for ROS-generating cellular factors induced by IGF-I pretreatment. As summarized in Fig. 2B, the COX-2–specific inhibitors NS-398 (10–100 μM) and SC58125 (1–10 μM), substantially attenuated the IGF-potentiated Zn^{2+} toxicity, whereas the COX-1 inhibitor SC560 (1–10 μM) did not. Neither the xanthine dehydrogenase inhibitor allopurinol (1 mM), the NADPH oxidase inhibitor DPI (1 μM), nor the NOS inhibitors N^G-monomethyl-L-arginine (1 mM) and N^G-nitro-L-arginine methyl ester (5 mM) repressed IGF-I–enhanced Zn^{2+} toxicity, despite the fact that these inhibitors except DPI were applied at millimolar levels (Fig. 2, C and D). Based on these results, we focused on the role of COX-2 in IGF-I–enhanced Zn^{2+} toxicity.

COX-2 Is a ROS-Generating Factor Induced by IGF-I Pretreatment. The need for a long-term (>12 h) preincubation with IGF-I to produce strong potentiation (Fig. 1C) suggested that cellular reprogramming, including new protein synthesis, is required for the IGF-I–induced potentiation of Zn^{2+} toxicity. In fact, cotreatment with cycloheximide or anisomycin during IGF-I pretreatment completely blocked the potentiating effect of IGF-I (Fig. 3, A and B). In contrast, the IGF-I–potentiated Zn^{2+} toxicity was barely affected when these inhibitors were applied after Zn^{2+} treatment (Fig. 3C).

We tested whether COX-1 and COX-2 were candidate ROS-generating factors induced by IGF-I pretreatment. Semiquantitative RT-PCR using [^{32}P]cytosine indicated that the transcription levels of COX-1 and -2 were gradually increased after treatment with 100 ng/ml IGF-I, although the induction of COX-1 was delayed and occurred at a relatively lower level than induction of COX-2. The increased expression of the COX-2 transcript peaked 10 to 12 h after the IGF-I treatment start and decreased gradually thereafter. At its peak, the expression level of COX-2 reached ~2.4-fold that of the control (Fig. 3D). The expression of the other ROS-generating enzymes, including xanthine dehydrogenase, NADPH oxidase ($p47^{phox}$, $gp91^{phox}$), and nNOS, were not significantly altered in the corresponding tests (data not shown).

In accordance with these results, Western blot analysis revealed that the level of COX-2 protein increased and peaked 12 to 24 h after treatment with 100 ng/ml IGF-I (Fig. 4A). In primary cortical cultures treated with 100 ng/ml IGF-I for 24 h, PGE_2 release was ~2.7-fold the basal level (Fig. 4B), indicating that the COX activity was enhanced after IGF-I treatment. Consistent with these results, immunocytological staining also revealed increased COX-2 expression in neuronal cells 24 h after the treatment with 100 ng/ml IGF-I (Fig. 4C), whereas COX-1 expression remained unchanged until 24 h after treatment with IGF-I (data not shown).

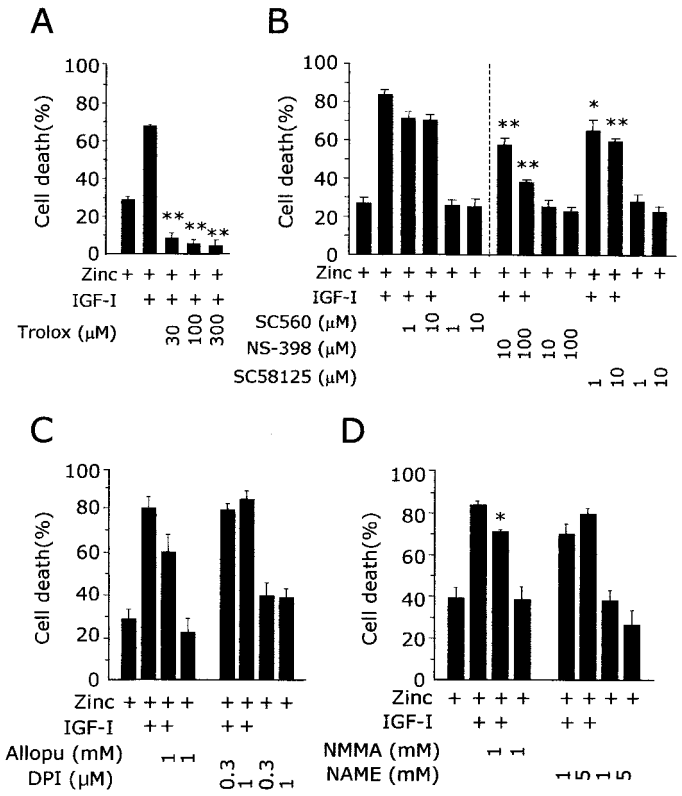

Fig. 2. The effects of ROS generating enzyme inhibitors on the IGF-I–induced potentiation of Zn^{2+} toxicity. A, Zn^{2+} toxicity potentiated by IGF-I was completely inhibited by trolox (30–300 μM) when applied after 80 μM Zn^{2+} treatment. However, treating the same doses of trolox for 12 h during IGF-I incubation was ineffective (data not shown). B–D, the COX-1–selective inhibitor SC560 (10 μM) did not suppress IGF-I–potentiated Zn^{2+} toxicity in cortical cultures, whereas the COX-2–selective inhibitors NS398 (10–100 μM) and SC58125 (10 μM) protected against increased cell death (B). The xanthine dehydrogenase inhibitor allopurinol (Allopu; 1 mM) (C), the NADPH oxidase inhibitor DPI (1 μM) (C), and the NOS inhibitors N^G-monomethyl-L-arginine (NMMA;1 mM) and N^G-nitro-L-arginine methyl ester (NAME; 5 mM) (D) were each tested. * and **, differences at the $p < 0.05$ and $p < 0.01$ levels, respectively, compared with Zn^{2+} + IGF-I (A–D). n = 8 to 12 in all cases.

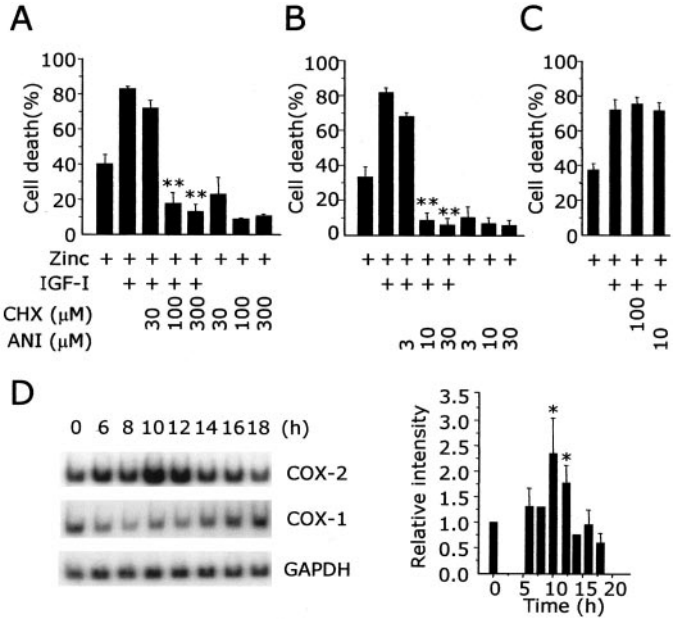

Fig. 3. Expression of COX-2 was induced by IGF-I. A–C, treatment of cycloheximide (CHX; 30–300 μM) or anisomycin (ANI; 3–30 μM) during pre-exposure to 100 ng/ml IGF-I blocked the potentiation effect (A and B). When they were applied after treating IGF-I, the potentiation effect was sustained (C). D, RT-PCR analysis of COX mRNA levels at various time points after 100 ng/ml IGF-I exposure (left). The expression of COX-2 was quantified by normalizing with GAPDH (right). * and **, differences at the $p < 0.05$ and $p < 0.01$ levels, respectively, compared with Zn^{2+} + IGF-I (A-C) or time 0 (D). n = 6 to 12 for A–C and n = 3 to 4 for D.

Arachidonic Acid Metabolism Is Involved in the IGF-I–Induced Potentiation of Zn^{2+} Toxicity. To further substantiate the hypothesis that increased COX-2 activity increases Zn^{2+} toxicity, we tested whether the exogenous supply of the COX-2 substrate AA affects Zn^{2+} toxicity. We found that pretreatment of cortical cultures with 100 ng/ml IGF-I doubled the cytotoxicity induced by different doses of AA alone (Fig. 5A), supporting the notion that the increased COX-2 expression in response to IGF-I pretreatment plays a role in cell death. The treatment of cortical cultures with 80 μM Zn^{2+} for 30 min and then 20 μM AA greatly enhanced cytotoxicity versus that induced by 80 μM Zn^{2+} alone (Fig. 5B). The Zn^{2+} toxicity enhancing effect of AA was similar to that of IGF-I preincubation (Fig. 1, B and C). Furthermore, the AA-induced potentiation of Zn^{2+} toxicity was effectively blocked by NS-398 in a dose-dependent manner (Fig. 5C). However, PGE_2 or 15-deoxy-12,14-PGJ_2, even at 30 μM, did not potentiate Zn^{2+}-induced cell death (Fig. 5D).

Next, we examined whether the COX-2–mediated potentiation of Zn^{2+}-toxicity is accompanied by enhanced oxidative stress; this was suggested by the observed protective effect of trolox (Fig. 2A). First, to monitor the intracellular ROS pressure, we chose GSH as a biochemical marker. At 3 h after treatment with 80 μM Zn^{2+}, followed by incubation with 20 μM AA, the level of intracellular GSH reduced to 78% of the control ($p < 0.05$, Newman-Keuls test). Likewise, 3 h after a 12-h pretreatment with 100 ng/ml IGF-I alone, or 3 h after a 12-h pretreatment with 100 ng/ml IGF-I followed by 80 μM Zn^{2+}, the intracellular GSH level decreased to 85% and 83% of the sham control level, respectively ($p < 0.05$, Newman-Keuls test). Furthermore, the intracellular GSH levels at 6 h after treating 80 μM Zn^{2+} followed by incubating 20 μM AA or at 6 h after a 12-h pretreatment with 100 ng/ml IGF-I followed by 80 μM Zn^{2+} reduced to 56% and 66% of the sham control level, respectively ($p < 0.01$ compared with either the sham control or 80 μM Zn^{2+} alone, Newman-Keuls test) (Fig. 6A). These results indicate that substantial ROS stress was produced in Zn^{2+}-treated primary cortical cultures pretreated with IGF-I. Cortical cultures consistently exposed to the GSH-depleting agent BSO (1 mM) for 12 h showed higher levels of cell death than those exposed to 80 μM Zn^{2+} alone. In this case, NS398 (10–100 μM) protected against cell death, although its effect was not profound (Fig. 6B).

ROS accumulation in cortical cells was visualized using the ROS-specific fluorescent dye, CM-H_2DCFDA. Cortical neurons pretreated with IGF-I for 12 h, followed by challenge with Zn^{2+}, showed markedly enhanced ROS production compared with neurons treated with IGF-I or Zn^{+} alone. Moreover, this increased ROS production was effectively blocked by 100 μM NS-398 (Fig. 7, A–E). We next tested whether the AA metabolism itself could cause ROS production. Cortical

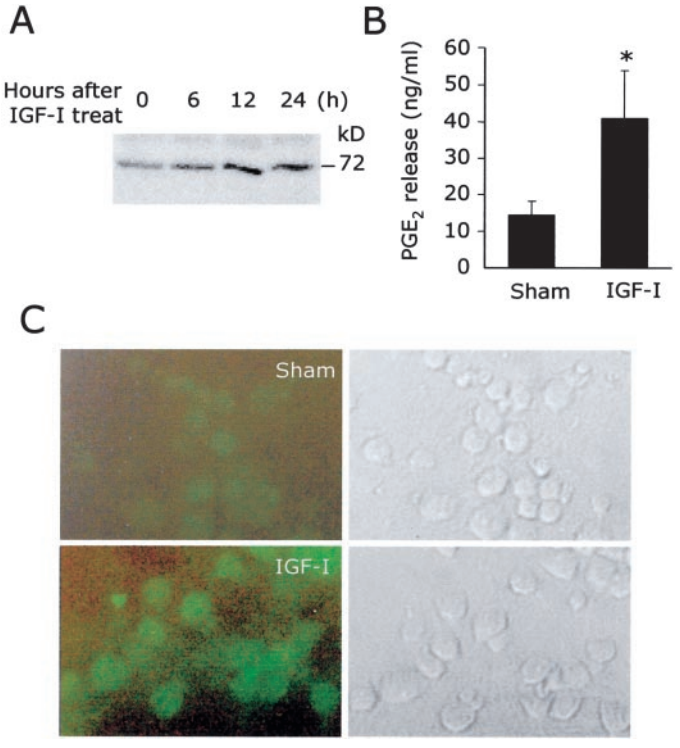

Fig. 4. Increases of COX-2 protein and COX activity after IGF-I pretreatment. A, Western blot analysis for COX-2 protein level in cortical culture at 6, 12, and 24 h after 100 ng/ml IGF-I treatment. B, COX activity was determined by measuring PGE_2 production in cortical cultures 24 h after treatment with 100 ng/ml IGF-I. C, photomicrographs showing anti-COX-2 immunoreactivity of the cortical culture 24 h after treatment with 100 ng/ml IGF-I (left) and paired phase contrast images (right). The large granule-like cells in the phase contrast images are neurons. Astrocytes lying on the culture plate are not clearly visible in these phase contrast images. *, difference at the $p < 0.05$ level compared with the sham control. $n = 3$ for A and C, and $n = 8$ for B.

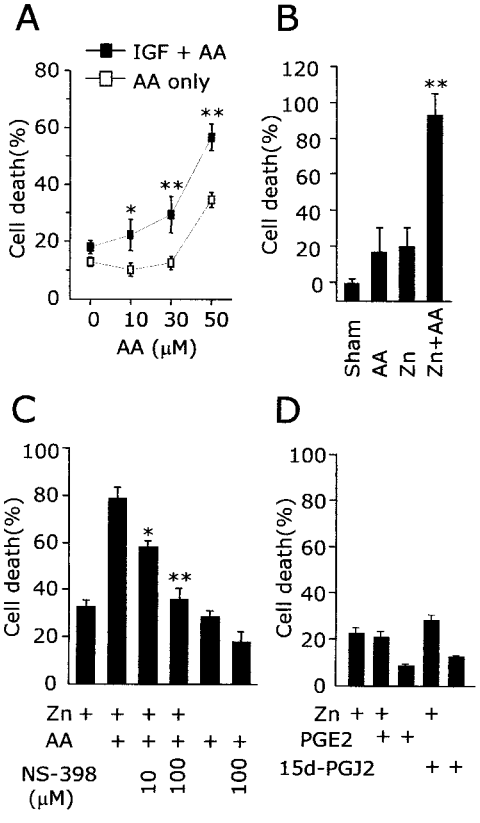

Fig. 5. Arachidonic acid mimicked the potentiating effect of IGF-I pretreatment. A, the cytotoxic effect of AA doubled when cortical cultures were exposed to 100 ng/ml of IGF-I for 12 h before treating AA. B, the addition of AA (20 μM) after treatment for 30 min with 80 μM Zn^{2+} (Zn + AA) strongly potentiated the cytotoxicity induced by 80 μM Zn^{2+} alone. C, the AA-induced potentiation of Zn^{2+} toxicity was blocked by NS-398 in a dose-dependent manner. D, PGE_2 (30 μM) and 15-deoxy-12,14-PGJ_2 (30 μM) did not mimic the potentiating effect of IGF-I on Zn^{2+} toxicity. * and **, differences at the $p < 0.05$ and $p < 0.01$ levels, respectively, compared with the paired control (A), Zn^{2+} (B) or Zn^{2+} +AA (C). $n = 8$ to 12 in all cases.

cultures treated with 80 μM Zn^{2+} for 30 min, followed by incubation with 20 μM AA showed markedly higher intracellular ROS levels, and this was also blocked by 100 μM NS-398 (Fig. 7, F–H). Cortical cultures challenged with 100 μM H_2O_2, a level that produces severe neuronal death 18 h after treatment (Cho et al., 2003), showed high ROS signs, and this was not suppressed by 100 μM NS-398 (Fig. 7, J and K). Therefore, the possibility that NS-398 has a nonspecific ROS-quenching effect can be excluded. Quantitative measurements of accumulated ROS in cortical neurons indicated that the level of ROS after treatment with IGF-I + Zn^{2+} reached >2.3-fold that of the sham control, which was returned to the control level by trolox (100 μM), NS-398 (100 μM), or SC58125 (10 μM) (Fig. 7L). As a whole, ROS generation in neurons challenged with 80 μM Zn^{2+} and then 20 μM AA is reminiscent of ROS generation in neurons insulted with 100 ng/ml IGF-I and then 80 μM Zn^{2+}, which supports the hypothesis that AA metabolism and ROS generation are involved in the IGF-I enhancement of Zn^{2+} toxicity.

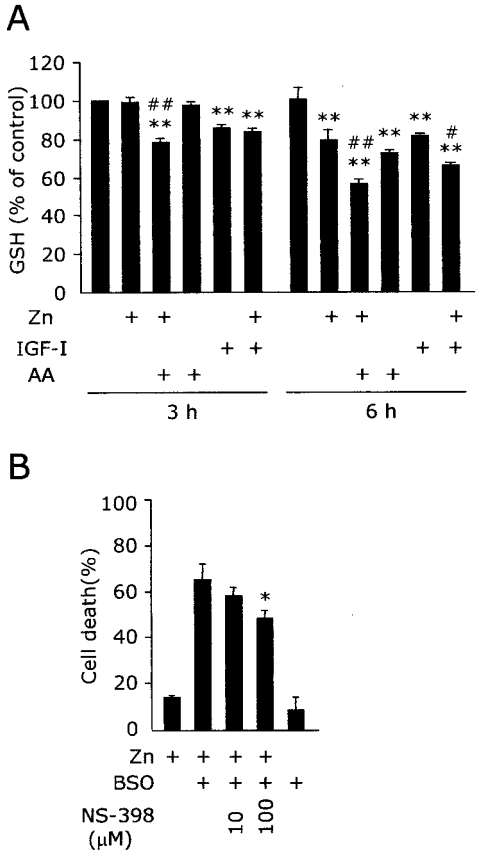

Fig. 6. Increased COX-2 activity reduced the intracellular GSH level. A, intracellular GSH levels in cortical cultures at 3 h after treatment with 80 μM Zn^{2+} only (Zn) or with 80 μM Zn^{2+} and 20 μM AA (Zn + AA) and at 3 h after a 12-h pretreatment with 100 ng/ml IGF-I alone (IGF-I) or after a 12-h pretreatment with 100 ng/ml IGF-I followed by treatment with 80 μM Zn^{2+} (IGF-I + Zn) or with Zn + AA, are presented (3 h). Intracellular GSH levels for similar sets were also measured at 6 h after treatment (6 h). B, 12 h of treatment with the GSH-depleting agent BSO (1 mM) greatly exacerbated the cytotoxicity induced by 80 μM Zn^{2+}. NS398 (10–100 μM) still afforded protection, although its effect was relatively weak. * and **, differences at the $p < 0.05$ and $p < 0.01$ levels, respectively, compared with the sham control. # and ##, differences at the $p < 0.05$ and $p < 0.01$ levels, respectively, compared with 80 μM Zn^{2+} alone. $n = 8$ to 10. Multiple comparisons were applied using analysis of variance followed by the Newman-Keuls test.

Discussion

This study demonstrates that COX-2 is responsible for the IGF-I induced potentiation of Zn^{2+} toxicity in primary cortical culture. The following findings support this. First, the COX-2–specific inhibitors, NS398 (10–100 μM) and SC58125 (10 μM), blocked IGF-I potentiated cell death (Fig. 2B). Second, COX activity was notably enhanced after exposure to IGF-I (Fig. 4B). The pretreatment of cortical cultures consistently with IGF-I markedly exacerbated the cytotoxicity induced by AA, the COX-2 substrate (Fig. 5A). Third, COX-2 expression was increased 12 to 24 h after IGF-I exposure (Figs. 3D and 4, A and C), which is in agreement with the need for new protein synthesis (Fig. 3, A–C) and the long-term (>12 h) incubation with IGF-I to produce its potentiation effects (Fig. 1C). Taken together, these results strongly support the hypothesis that COX-2 is responsible for the IGF-I–induced potentiation of Zn^{2+} toxicity in primary cortical culture.

We found that the Zn^{2+} treatment in the presence of increased COX-2 activity produced a substantial increase in the level of intracellular ROS (Figs. 6 and 7). To explain the results of our study, we propose the following model. COX-2 enzyme has both oxygenase activity, which uses molecular oxygen and peroxidase activity, which reduces hydroperoxides (Eling et al., 1986; Kukreja et al., 1986; Lu et al., 1999). The conversion of one molecule of AA to PGs by the sequential action of the oxygenase and peroxidase activities of COX-2 requires two oxygen molecules and two electrons (Smith et al., 1996). Therefore, as COX-2 activity increases, cells require more cellular NAD(P)H or GSH, which results in the gradual consumption of the cell's reducing power, unless new reducing factors are introduced. The concepts incorporated into this model are summarized in Fig. 8. As this model explains, cortical cells with enhanced COX-2 activity may accumulate intracellular ROS, even when the cells are challenged by weak ROS-generating conditions, such as treatment with 80 μM Zn^{2+} for 30 min. In agreement with this speculation, our biochemical data indicate that the level of intracellular GSH rapidly reduced in cortical cultures pretreated with IGF-I and followed by Zn^{2+} challenge and in cortical cultures treated with Zn^{2+} and followed by AA (Fig. 6A). Cortical neurons challenged with 10 μM Fe^{2+} and 20 μM AA greatly increased ROS production, which was suppressed by NS-398 (data not shown). To the best of our knowledge, this model is the first to explain how enhanced COX-2 activity directly contributes to the generation of ROS stress. Cells with low reducing power may be vulnerable to subsequent ROS stress, as is the case for cellular processes exposed to low doses of free Zn^{2+}. Accumulated ROS in cells oxidizes cellular substrates, such as proteins, lipids, and DNA, which may result in cell death (Kim et al., 1999a,b). In the case of a Zn^{2+} overload, GSH depletion might be accelerated, and the proper maintenance of thiol homeostasis is likely to be disrupted (Kim et al., 2003a). On the other hand, reactive oxygen radicals may interact with thiols and generate cytotoxic thiyl radicals and thiyl free radical metabolites (Eling et al., 1986; Takeuchi et al., 1991).

IGF-I–induced potentiation of Zn^{2+} toxicity was completely blocked by the protein synthesis inhibitors cycloheximide or anisomycin only when they were applied during the IGF-I pretreatment (Fig. 3, A–C). Thus, de novo protein

synthesis was involved in the IGF-I–induced potentiation, as it was in BDNF-induced processes (Gwag et al., 1995; Ryu et al., 1999; Fryer et al., 2000). However, unlike BDNF-induced potentiation, NOS inhibitors did not block the IGF-I–induced potentiation of Zn^{2+} toxicity (Fig. 2D), and IGF-I pretreatment barely changed the expression of nNOS in cortical cultures (data not shown). Kim et al. (2002) reported that the prolonged incubation of primary cortical cultures with BDNF rapidly and substantially induced the expression of NADPH oxidase, which caused superoxide-mediated neuronal injury. Our semiquantitative RT-PCR study using [^{32}P]cytosine indicated that the level of $p47^{phox}$ and $gp91^{phox}$ expression in cortical cultures, treated for 18 h with 100 ng/ml IGF-I, was barely changed (data not shown). These results suggest that the detailed mechanism underlying the IGF-I–induced potentiation of Zn^{2+} toxicity is distinct from that involved in BDNF-induced potentiation.

NS398 (10 μM) and SC58125 (10 μM) significantly, but partially, suppressed IGF-potentiated Zn^{2+} toxicity, although 100 μM NS398 strongly suppressed this potentiated cell death (Fig. 2B). Several possibilities are conceivable. First, although COX-2 is a critical factor for the process, additional factors that are induced by IGF-I may play a role in IGF-potentiated Zn^{2+} toxicity. Second, Zn^{2+} influx into neurons caused by treating with 80 μM Zn^{2+} may elicit multiple arrays of cytotoxic signals along with the activation of the COX-2–related pathway. There is a wealth of evidence that free Zn^{2+} disrupts various aspects of the intracellular physiology, including the induction and activation of NADPH oxidase and energy failure (Noh and Koh, 2000; Sheline et al., 2000). Third, COX-1 could add functionally to COX activity enhancement. The IC_{50} for the inhibition of COX-2 by NS-398 is 1 to 2 μM in cell free assays. In general, however, much higher doses of this inhibitor are used in studies with intact cells. The IC_{50} for the inhibition of COX-1 by NS-398 is reported to be >100 μM (DeWitt, 1999). NS-398 is known to

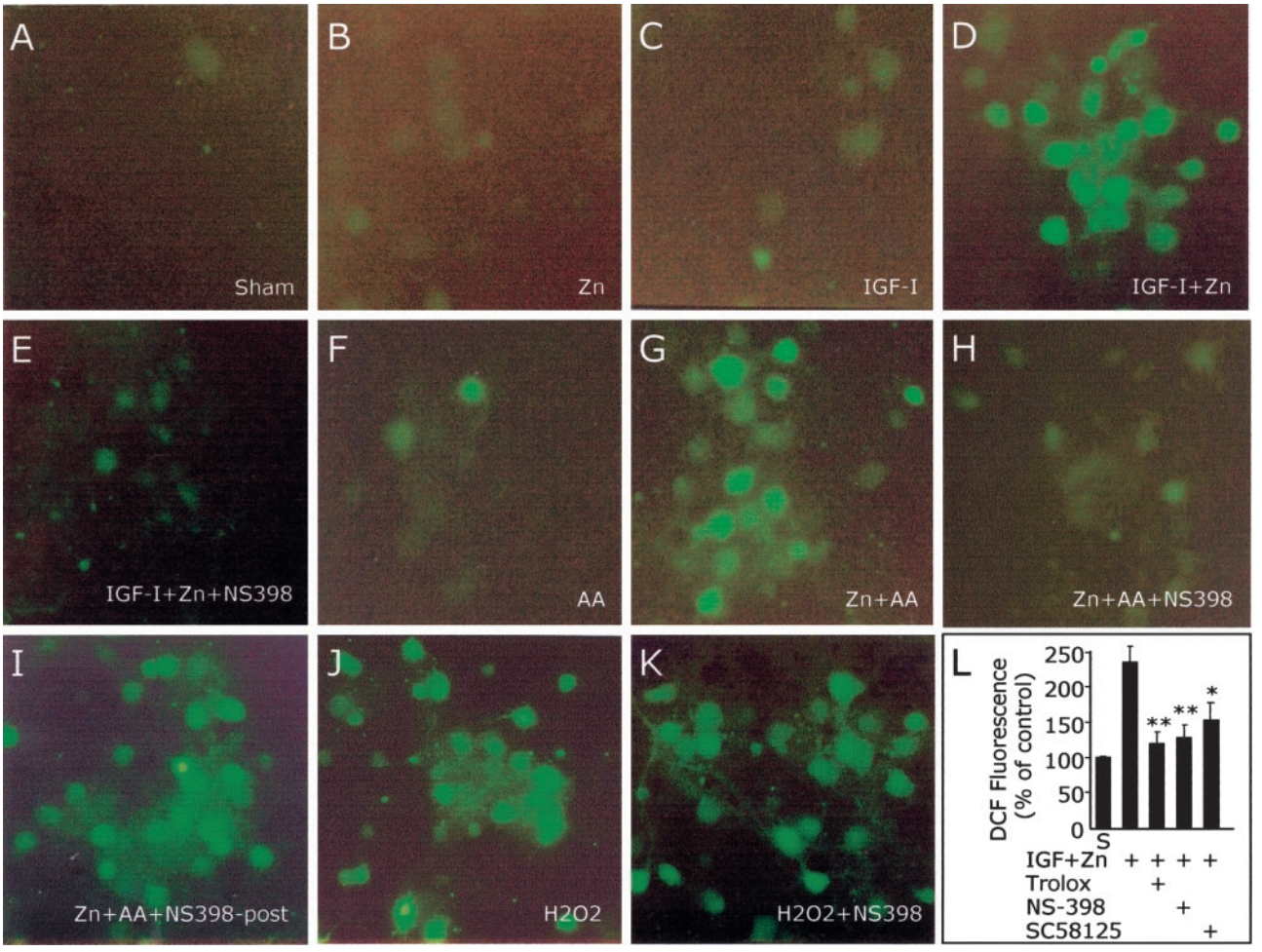

Fig. 7. Visualization by CM-H_2DCFDA of ROS generation involved in IGF-I potentiation and AA metabolism. A–E, ROS generation in cortical cultures at 4 h after a 12-h pretreatment with 100 ng/ml IGF-I (IGF-I; C), 80 μM Zn^{2+} (for 30 min) (Zn; B), or a 12-h pretreatment with 100 ng/ml IGF-I followed by 80 μM Zn^{2+}-treatment (IGF-I + Zn; D). NS-398 (100 μM) blocked the ROS rise in cortical neurons challenged with IGF-I + Zn (IGF-I+Zn+NS398; E). F–I, ROS levels in cortical neurons at 4 h after treatment with 20 μM AA (F) or treatment with 80 μM Zn^{2+} followed by 20 μM AA (Zn+AA; G). The rise of ROS accumulation in Zn + AA was inhibited by 100 μM NS-398 (Zn+AA+NS398; H), which was comparable with that observed for IGF-I + Zn + NS-398 (E). NS-398 (100 μM) application for 30 min before CM-H_2DCFDA application did not suppress ROS generation (Zn+AA+NS398-post; I). J–K, ROS levels in cortical neurons challenged with 100 μM H_2O_2 (H_2O_2; J). Coincubation of 100 μM H_2O_2 with NS-398 did not suppress the rise in ROS levels (H_2O_2+NS398; K). These experiments (A–K) were repeated more than three times, and representative photomicrographs are presented. L, ROS levels in cortical cultures prepared in 24-well plates were quantified after staining with CM-H_2DCFDA. ROS levels in IGF-I (100 ng/ml)-pretreated cortical cultures at 4 h after treatment with 80 μM Zn^{2+} reached a level that was >2.3-fold higher than that in the sham control. This rise in ROS level was brought back to the control level after treating with 100 μM trolox, 100 μM NS-398, or 10 μM SC58125 ($p < 0.05$, $n = 24$ spots from eight wells in each group). **, difference at the $p < 0.01$ level compared with the sham control.

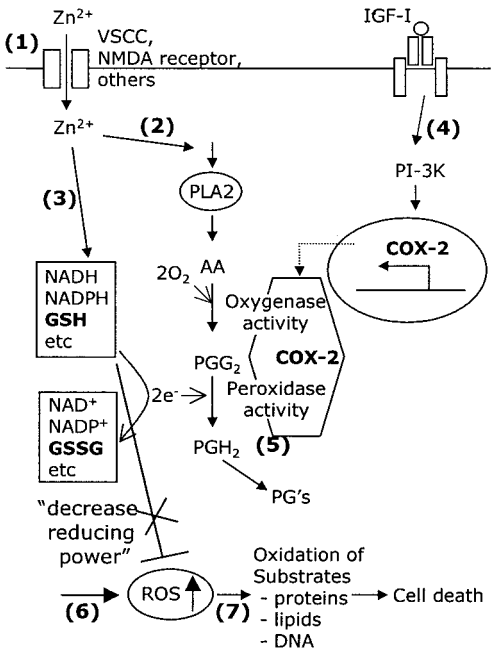

Fig. 8. A hypothetical model for the role of COX-2 in ROS generation and potentiated cell death. COX-2, which has both oxygenase and peroxidase activities, uses two oxygen molecules and two electrons to convert one molecule of AA to PGs. NADH, NADPH, or GSH may donate the required electrons as a result of their oxidation to NAD^+, $NADP^+$, or GSSG, respectively. Therefore, the increase in COX-2 activity caused by either enhanced COX- expression or an increase in the supply of its substrate, AA, depletes the cellular reservoirs of NADH, NADPH, or GSH, resulting in a decrease in the cell's reducing power. In this cellular context, cortical neurons may not be able to cope with weak ROS stress such as a Zn^{2+} insult, and thus cell death is enhanced. This model emphasizes not only that the induction of COX-2 by IGF-I pretreatment potentiates cell death but also that enhanced COX-2 activity contributes to the accumulation of ROS. This model does not necessarily eliminate the possibility that IGF-I affects the cell death induced by other cytotoxic molecules. Selected references for each step are indicated in the diagram: **(1)** Sensi et al., 1997; **(2)** Noh et al., 1999; **(3)** Noh and Koh, 2000; Kim et al. 2003a; **(4)** Ryu et al., 1999; **(5)** Smith et al., 1996; **(6)** Kim et al., 1999a; **(7)** Kim et al., 1999b. VSCC, voltage gated Ca^{2+} channel; PLA2, phospholipase A2; GSSG, oxidized glutathione (GSH); PI3-K, phosphatidylinositol 3-kinase.

exhibit a 1000-fold selectivity for the inhibition of COX-2 over COX-1 (Gierse et al., 1995). Despite these properties of NS-398 and the failure of the COX-1–selective inhibitor SC560 (10 μM) to suppress IGF-potentiated Zn^{2+} toxicity (Fig. 2B), the results of our study do not exclude the possibility that 100 μM NS398 partially inhibits COX-1 and thus contributes to the inhibition of potentiated cell death.

In summary, IGF-I pretreatment makes primary cortical neurons highly vulnerable to subsequent weak cytotoxic insults. The underlying mechanism involves the induction of COX-2, and the loss of the cell's reducing power. Subsequent weak ROS insults may be highly detrimental to viability. The results of our study raise the possibility that appropriately controlled intervention may be necessary to avoid the potentially exacerbating effects of IGF-I in the treatment of neuropathological conditions.

Acknowledgments

This study was supported by a grant to P.-L.H. from the Neurobiology Research Program of the Ministry of Science and Technology, Republic of Korea.

References

Assaf SY and Chung SH (1984) Release of endogenous Zn^{2+} from brain tissue during activity. *Nature (Lond)* **308:**734–736.
Behrens MM, Strasser U, Lobner D, and Dugan LL (1999) Neurotrophin-mediated potentiation of neuronal injury. *Microsc Res Tech* **45:**276–284.
Boldyrev AA, Carpenter DO, Huentelman MJ, Peters CM, and Johnson P (1999) Sources of reactive oxygen species production in excitotoxin- stimulated cerebellar granule cells. *Biochem Biophys Res Commun* **256:**320–324.
Candelario-Jalil E, Ajamieh HH, Sam S, Martinez G, and Leon Fernandez OS (2000) Nimesulide limits kainate-induced oxidative damage in the rat hippocampus. *Eur J Pharmacol* **390:**295–298.
Cho I-H, Im J-Y, Kim D, Kim K-S, Lee J-K, and Han P-L (2003) Protective effects of extracellular glutathione against Zn^{2+}-induced cell death in vitro and in vivo. *J Neurosci Res* **74:**736–743.
DeWitt DL (1999) Cox-2-selective inhibitors: the new super aspirins. *Mol Pharmacol* **55:**625–631.
Eling TE, Curtis JF, Harman LS, and Mason RP (1986) Oxidation of glutathione to its thiyl free radical metabolite by prostaglandin H synthase. A potential endogenous substrate for the hydroperoxidase. *J Biol Chem* **261:**5023–5028.
Estus S, Zaks WJ, Freeman RS, Gruda M, Bravo R, and Johnson EM (1994) Altered gene expression in neurons during programmed cell death: identification of c-jun as necessary for neuronal apoptosis. *J Cell Biol* **127:**1717–1727.
Frederickson CJ, Hernandez MD, Goik SA, Morton JD, and McGinty JF (1988) Loss of zinc staining from hippocampal mossy fibers during kainic acid induced seizures: a histofluorescence study. *Brain Res* **446:**383–386.
Fryer HJ, Wolf DH, Knox RJ, Strittmatter SM, Pennica D, O'Leary RM, Russell DS and Kalb RG (2000) Brain-derived neurotrophic factor induces excitotoxic sensitivity in cultured embryonic rat spinal motor neurons through activation of the phosphatidylinositol 3-kinase pathway. *J Neurochem* **74:**582–595.
Gierse JK, Hauser SD, Creely DP, Koboldt C, Rangwala SH, Isakson PC, and Seibert K (1995) Expression and selective inhibition of the constitutive and inducible forms of human cyclo-oxygenase. *Biochem J* **305:**479–484.
Glazner GW and Mattson MP (2000) Differential effects of BDNF, ADNF9, and TNFalpha on levels of NMDA receptor subunits, calcium homeostasis and neuronal vulnerability to excitotoxicity. *Exp Neurol* **161:**442–452.
Greenlund LJ, Deckwerth TL, and Johnson EM Jr (1995) Superoxide dismutase delays neuronal apoptosis: a role for reactive oxygen species in programmed neuronal death. *Neuron* **14:**303–315.
Guan J, Miller OT, Waugh KM, McCarthy DC, and Gluckman PD (2001) Insulin-like growth factor-1 improves somatosensory function and reduces the extent of cortical infarction and ongoing neuronal loss after hypoxia-ischemia in rats. *Neuroscience* **105:**299–306.
Gunasekar PG, Borowitz JL, and Isom GE (1998) Cyanide-induced generation of oxidative species: involvement of nitric oxide synthase and cyclooxygenase-2. *J Pharmacol Exp Ther* **285:**236–241.
Gwag BJ, Koh JY, Chen MM, Dugan LL, Behrens MM, Lobner D, and Choi DW (1995) BDNF or IGF-I potentiates free radical-mediated injury in cortical cell cultures. *Neuroreport* **7:**93–96.
Hool LC and Arthur PG (2002) Decreasing cellular hydrogen peroxide with catalase mimics the effects of hypoxia on the sensitivity of the L-type Ca^{2+} channel to beta-adrenergic receptor stimulation in cardiac myocytes. *Circ Res* **91:**601–609.
Ishikawa Y, Ikeuchi T, and Hatanaka H (2000) Brain-derived neurotrophic factor accelerates nitric oxide donor-induced apoptosis of cultured cortical neurons. *J Neurochem* **75:**494–502.
Kim D, Joe CO, and Han P-L (2003a) Extracellular and intracellular glutathione protects astrocytes from Zn^{2+}-induced cell death. *Neuroreport* **14:**187–190.
Kim EY, Koh JY, Kim YH, Sohn S, Joe E, and Gwag BJ (1999a) Zn^{2+} entry produces oxidative neuronal necrosis in cortical cell cultures. *Eur J Neurosci* **11:**327–334.
Kim HJ, Hwang JJ, Behrens MM, Snider BJ, Choi DW, and Koh JY (2003b) TrkB mediates BDNF-induced potentiation of neuronal necrosis in cortical culture. *Neurobiol Dis* **214:**110–119.
Kim SH, Won SJ, Sohn S, Kwon HJ, Lee JY, Park JH, and Gwag BJ (2002) Brain-derived neurotrophic factor can act as a pronecrotic factor through transcriptional and translational activation of NADPH oxidase. *J Cell Biol* **159:**821–831.
Kim YH, Kim EY, Gwag BJ, Sohn S, and Koh JY (1999b) Zinc-induced cortical neuronal death with features of apoptosis and necrosis: mediation by free radicals. *Neuroscience* **89:**175–182.
Koh JY, Gwag BJ, Lobner D, and Choi DW (1995) Potentiated necrosis of cultured cortical neurons by neurotrophins. *Science (Wash DC)* **268:**573–575.
Koh JY, Suh SW, Gwag BJ, He YY, Hsu CY, and Choi DW (1996) The role of zinc in selective neuronal death after transient global cerebral ischemia. *Science (Wash DC)* **272:**1013–1016.
Kukreja RC, Kontos HA, Hess ML, and Ellis EF (1986) PGH synthase and lipoxygenase generate superoxide in the presence of NADH or NADPH. *Circ Res* **59:**612–619.
Kyrkanides S, Moore AH, Olschowka JA, Daeschner JC, Williams JP, Hansen JT, and Kerry O'Banion M (2002) Cyclooxygenase-2 modulates brain inflammation-related gene expression in central nervous system radiation injury. *Mol Brain Res* **104:**159–169.
Lee J-K, Park J, Lee Y-D, Lee S-H, and Han P-L (1999) Distinct localization of SAPK isoforms in neurons of adult mouse brain implies multiple signaling modes of SAPK pathway. *Mol Brain Res* **70:**116–124.
Lee JY, Cole TB, Palmiter RD, Suh SW, and Koh JY (2002) Contribution by synaptic zinc to the gender-disparate plaque formation in human Swedish mutant APP transgenic mice. *Proc Natl Acad Sci USA* **99:**7705–7710.
Lobner D and Ali C (2002) Mechanisms of bFGF and NT-4 potentiation of necrotic neuronal death. *Brain Res* **954:**42–50.
Lu G, Tsai AL, Van Wart HE, and Kulmacz RJ (1999) Comparison of the peroxidase

reaction kinetics of prostaglandin H synthase-1 and -2. *J Biol Chem* **274:**16162–16167.
Mahadev K, Zilbering A, Zhu L, and Goldstein BJ (2001) Insulin-stimulated hydrogen peroxide reversibly inhibits protein-tyrosine phosphatase 1b in vivo and enhances the early insulin action cascade. *J Biol Chem* **276:**21938–21942.
Nabeshima T and Yamada K (2000) Neurotrophic factor strategies for the treatment of Alzheimer disease. *Alzheimer Dis Assoc Disord* **14:**S39–S46.
Nakayama M, Uchimura K, Zhu RL, Nagayama T, Rose ME, Stetler RA, Isakson PC, Chen J, and Graham SH (1998) Cyclooxygenase-2 inhibition prevents delayed death of CA1 hippocampal neurons following global ischemia. *Proc Natl Acad Sci USA* **95:**10954–10959.
Nogawa S, Zhang F, Ross ME, and Idecola C (1997) Cyclo-oxygenase-2 gene expression in neurons contributes to ischemic brain damage. *J Neurosci* **17:**2746–2755.
Noh KM, Kim YH, and Koh JY (1999) Mediation by membrane protein kinase C of zinc-induced oxidative neuronal injury in mouse cortical cultures. *J Neurochem* **72:**1609–1616.
Noh KM and Koh JY (2000) Induction and activation by zinc of NADPH oxidase in cultured cortical neurons and astrocytes. *J Neurosci* **20:**RC111.
Namiki J, Kojima A, and Tator CH (2000) Effect of brain-derived neurotrophic factor, nerve growth factor and neurotrophin-3 on functional recovery and regeneration after spinal cord injury in adult rats. *J Neurotrauma* **17:**1219–1231.
Prehn JH (1996) Marked diversity in the action of growth factors on *N*-methyl-D-aspartate-induced neuronal degeneration. *Eur J Pharmacol* **306:**81–88.
Rudge JS, Mather PE, Pasnikowski EM, Cai N, Corcoran T, Acheson A, Anderson K, Lindsay RM, and Wiegand SJ (1998) Endogenous BDNF protein is increased in adult rat hippocampus after a kainic acid induced excitotoxic insult but exogenous BDNF is not neuroprotective. *Exp Neurol* **149:**398–410.
Ryu BR, Ko HW, Jou I, Noh JS, and Gwag BJ (1999) Phosphatidylinositol 3-kinase-mediated regulation of neuronal apoptosis and necrosis by insulin and IGF-I. *J Neurobiol* **39:**536–546.
Samdani AF, Newcamp C, Resink A, Facchinetti F, Hoffman BE, Dawson VL, and Dawson TM (1997) Differential susceptibility to neurotoxicity mediated by neurotrophins and neuronal nitric oxide synthase. *J Neurosci* **17:**4633–4641.
Sensi SL, Canzoniero LM, Yu SP, Ying HS, Koh JY, Kerchner GA, and Choi DW (1997) Measurement of intracellular free zinc in living cortical neurons: routes of entry. *J Neurosci* **17:**9554–9964.
Sheline CT, Behrens MM, and Choi DW (2000) Zinc-induced cortical neuronal death: contribution of energy failure attributable to loss of NAD^+ and inhibition of glycolysis. *J Neurosci* **20:**3139–3146.
Small DL, Murray CL, Mealing GA, Poulter MO, Buchan AM, and Morley P (1998) Brain derived neurotrophic factor induction of *N*-methyl-D-aspartate receptor subunit NR2A expression in cultured rat cortical neurons. *Neurosci Lett* **252:**211–214.
Smith WL, Garavito RM, and DeWitt DL (1996) Prostaglandin endoperoxide H synthases (cyclooxygenases)-1 and -2. *J Biol Chem* **271:**33157–33160.
Suh SW, Chen JW, Motamedi M, Bell B, Listiak K, Pons NF, Danscher G, and Frederickson CJ (2000) Evidence that synaptically-released zinc contributes to neuronal injury after traumatic brain injury. *Brain Res* **852:**268–273.
Takeuchi Y, Morii H, Tamura M, Hayaishi O, and Watanabe Y (1991) A possible mechanism of mitochondrial dysfunction during cerebral ischemia: inhibition of mitochondrial respiration activity by arachidonic acid. *Arch Biochem Biophys* **289:**33–38.
Vane JR, Bakhle YS, and Botting RM (1998) Cyclooxygenases 1 and 2. *Annu Rev Pharmacol Toxicol* **38:**97–120.
Won SJ, Park EC, Ryu BR, Ko HW, Sohn S, Kwon HJ, and Gwag BJ (2000) NT-4/5 exacerbates free radical-induced neuronal necrosis in vitro and in vivo. *Neurobiol Dis* **7:**251–259.
Wu D and Pardridge WM (1999) Neuroprotection with noninvasive neurotrophin delivery to the brain. *Proc Natl Acad Sci USA* **96:**254–259.

Address correspondence to: Dr. Pyung-Lim Han, Ewha Institute of Neuroscience, Ewha Womans University School of Medicine, 70 Jongno-6-Ga, Jongno-Gu, Seoul, 110-783, Republic of Korea. E-mail: plhan@ewha.ac.kr